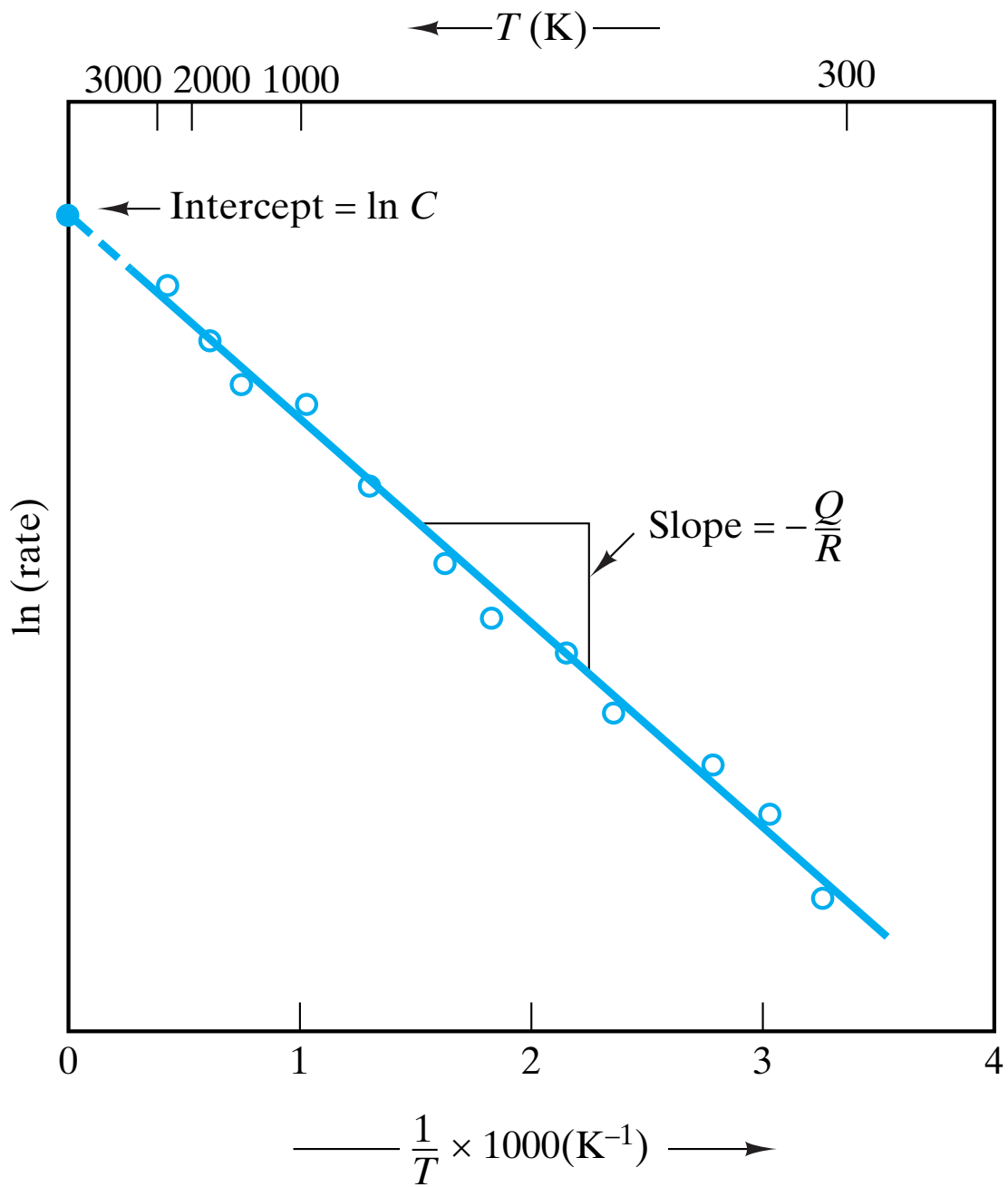


# CHAPTER 5

## Diffusion



*In addition to superconductivity and high melting point which lead to various important industrial applications, niobium is a metal which forms oxide coatings readily by the interdiffusion of oxygen and niobium atoms near the metal surface. Jewelry manufacturers use this fact to produce colorful earring designs. (Courtesy of Teledyne Wah Chang, Albany, Oregon.)*



**Figure 5-1** Typical Arrhenius plot of data compared to Equation 5.2. The slope equals  $-Q/R$  and the intercept (at  $1/T = 0$ ) is  $\ln C$ .

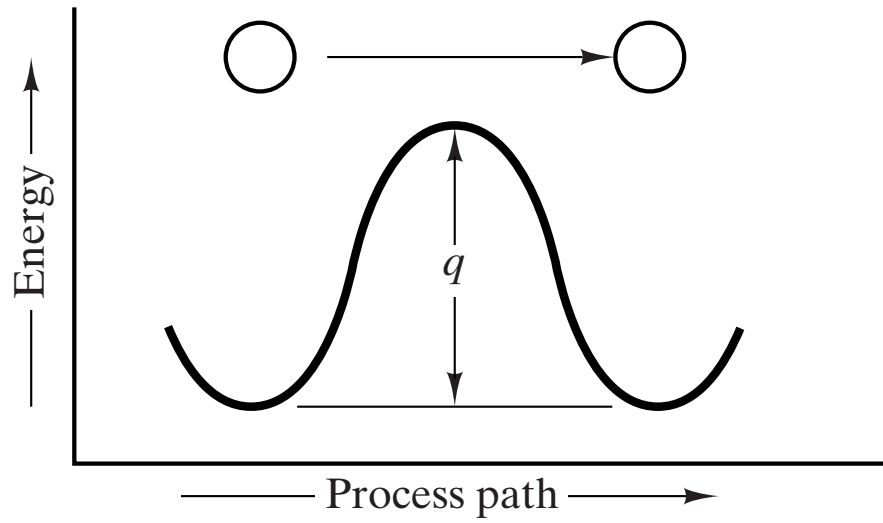


**Figure 5-2** *Process path showing how an atom must overcome an activation energy,  $q$ , to move from one stable position to a similar adjacent position.*

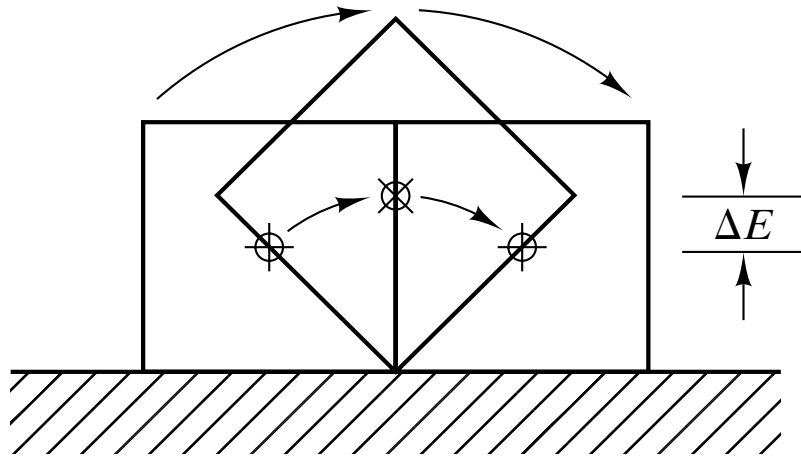


**Figure 5-3** Simple mechanical analog of the process path of Figure 5-2. The box must overcome an increase in potential energy,  $\Delta E$ , in order to move from one stable position to another.

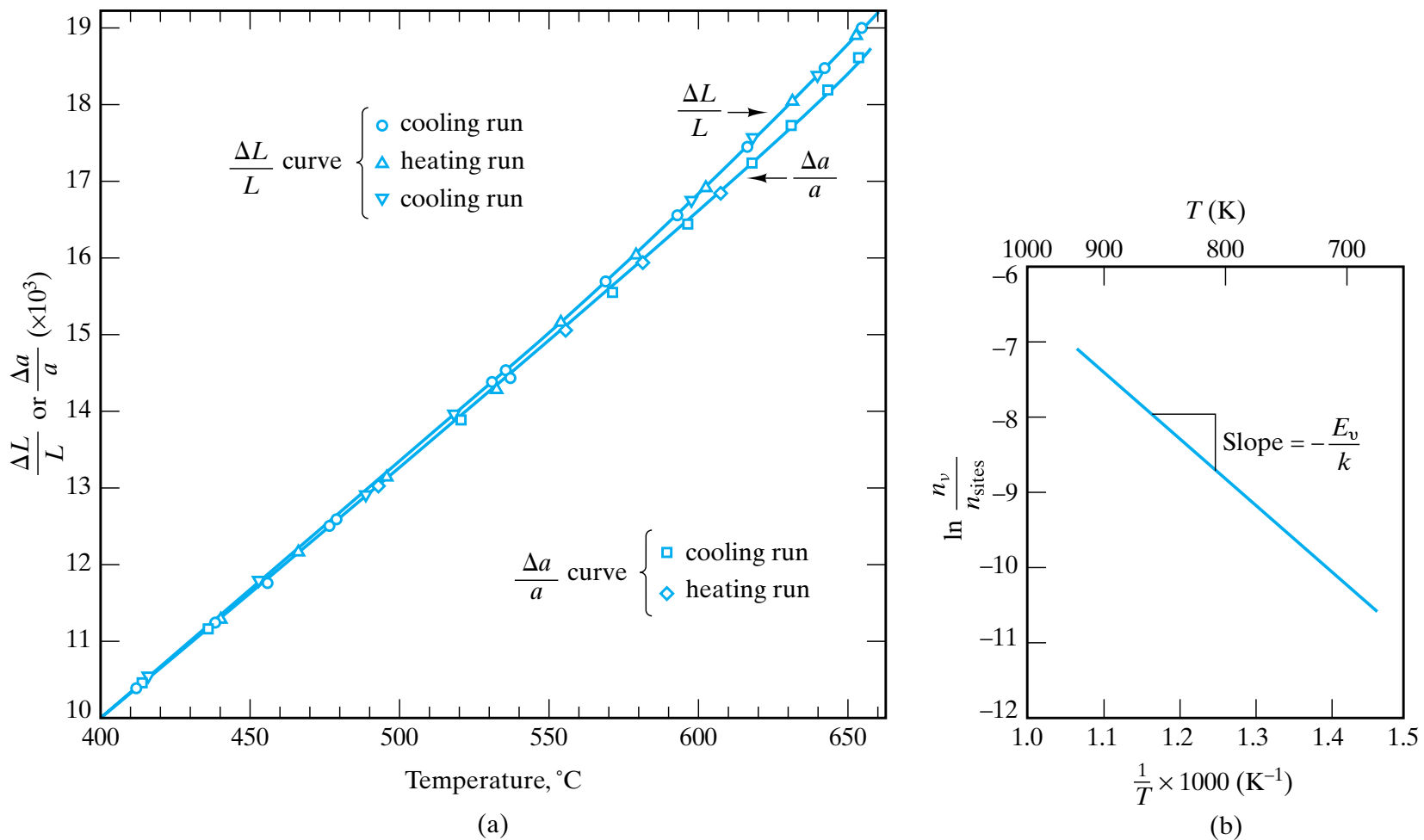


**Figure 5-4** (a) The overall thermal expansion ( $\Delta L/L$ ) of aluminum is measurably greater than the lattice parameter expansion ( $\Delta a/a$ ) at high temperatures because vacancies are produced by thermal agitation. (b) A semilog (Arrhenius-type) plot of  $\ln$  (vacancy concentration) versus  $1/T$  based on the data of part (a). The slope of the plot ( $-E_v/k$ ) indicates that 0.76 eV of energy is required to create a single vacancy in the aluminum crystal structure. (After P. G. Shewmon, *Diffusion in Solids*, McGraw-Hill Book Company, New York, 1963.)

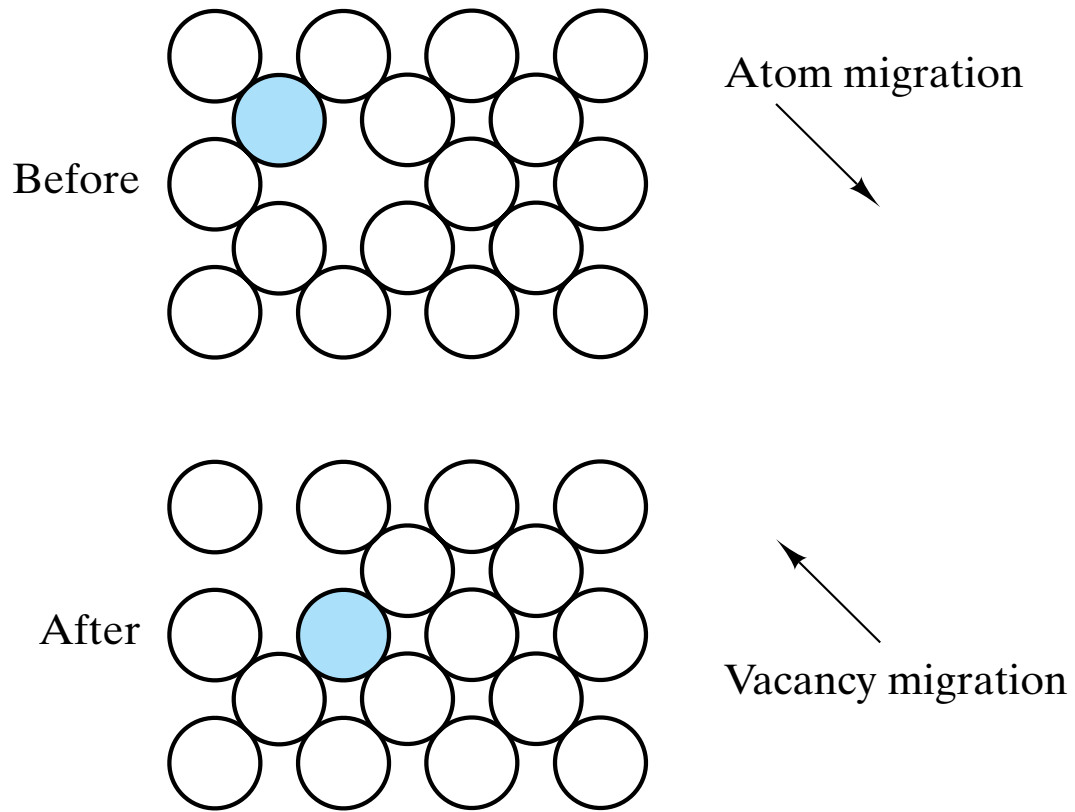


**Figure 5-5** Atomic migration occurs by a mechanism of vacancy migration. Note that the overall direction of material flow (the atom) is opposite to the direction of vacancy flow.

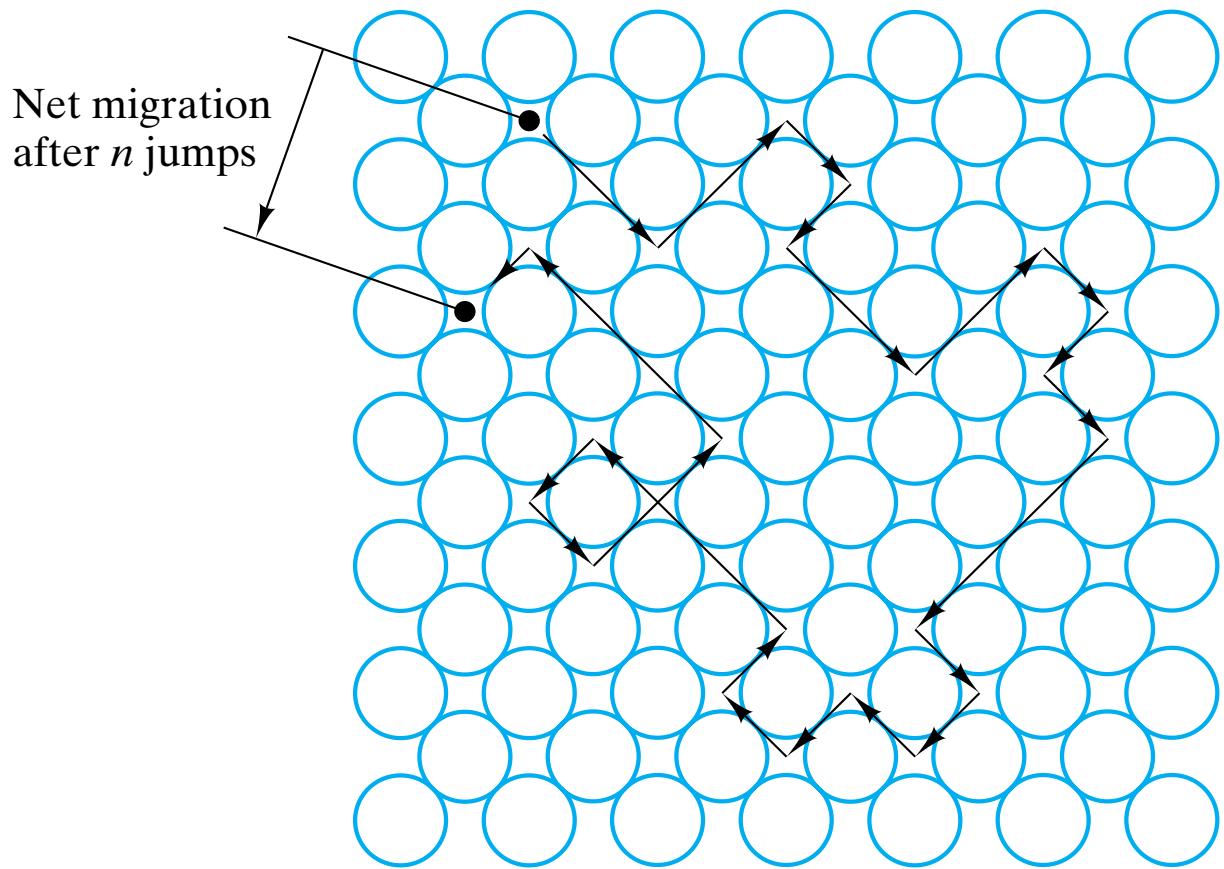


**Figure 5-6** Diffusion by an interstitialcy mechanism illustrating the random walk nature of atomic migration.

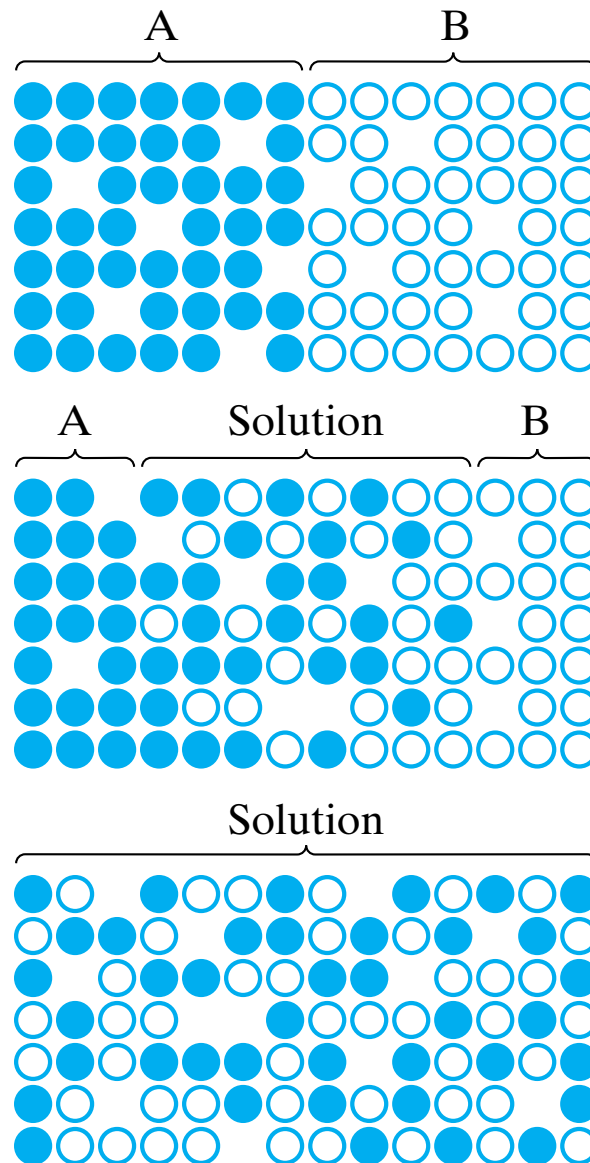


**Figure 5-7** *The interdiffusion of materials A and B. Although any given A or B atom is equally likely to “walk” in any random direction (see Figure 5-6), the concentration gradients of the two materials can result in a net flow of A atoms into the B material, and vice versa. (From W. D. Kingery, H. K. Bowen, and D. R. Uhlmann, Introduction to Ceramics, 2nd ed., John Wiley & Sons, Inc., New York, 1976.)*

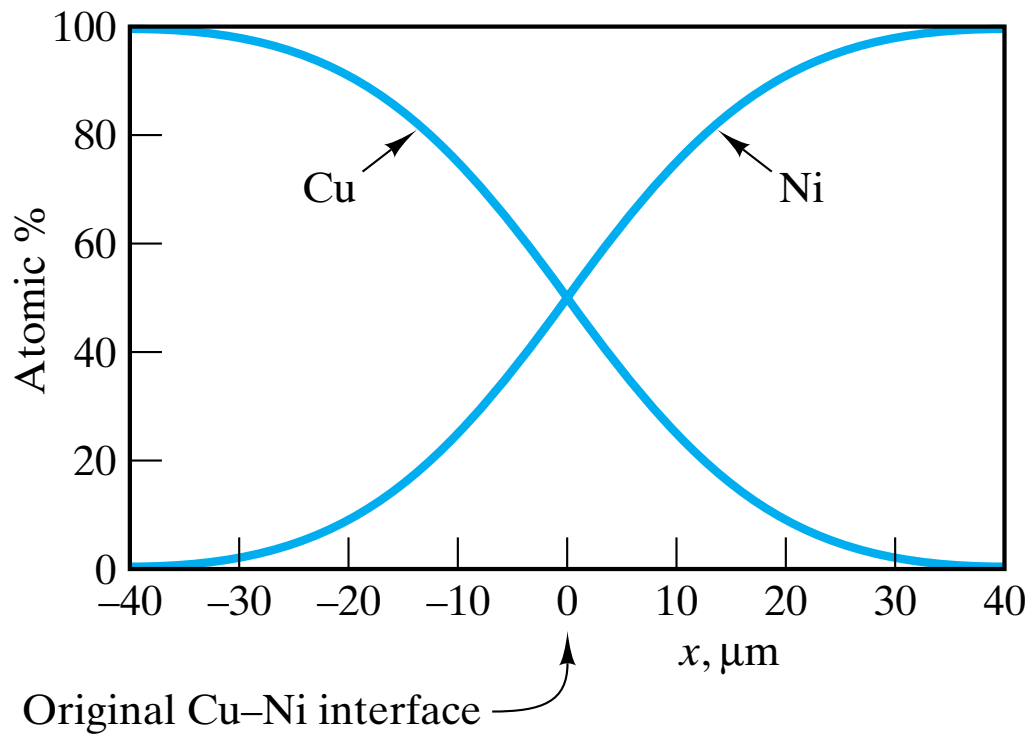


**Figure 5-8** *The interdiffusion of materials on an atomic scale was illustrated in Figure 5-7. A comparable example on the microscopic scale is this interdiffusion of copper and nickel.*

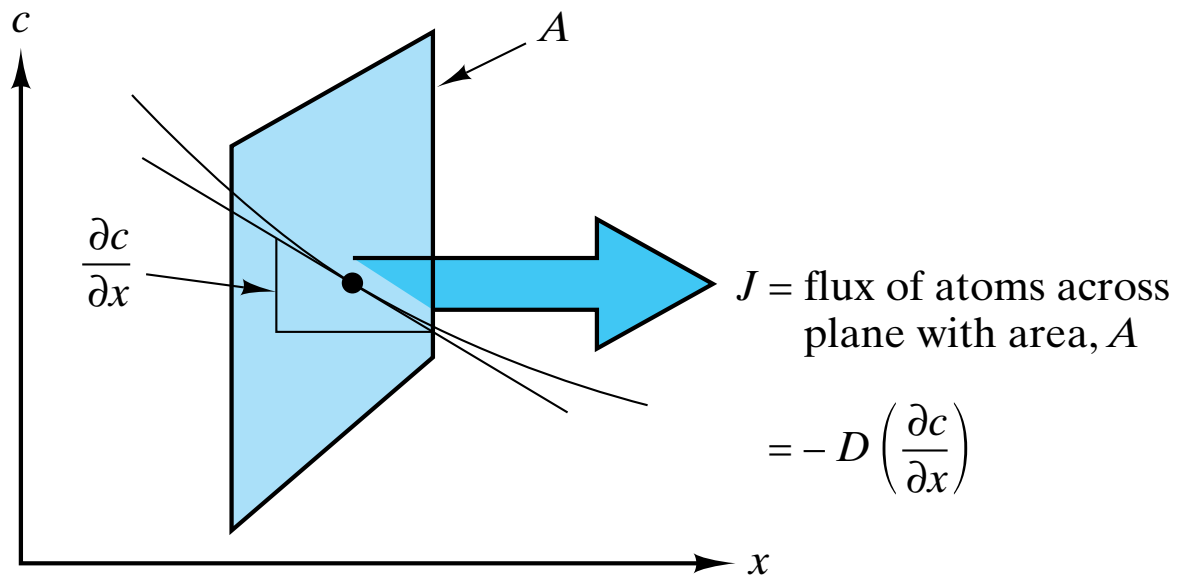


**Figure 5-9** Geometry of Fick's first law (Equation 5.8).

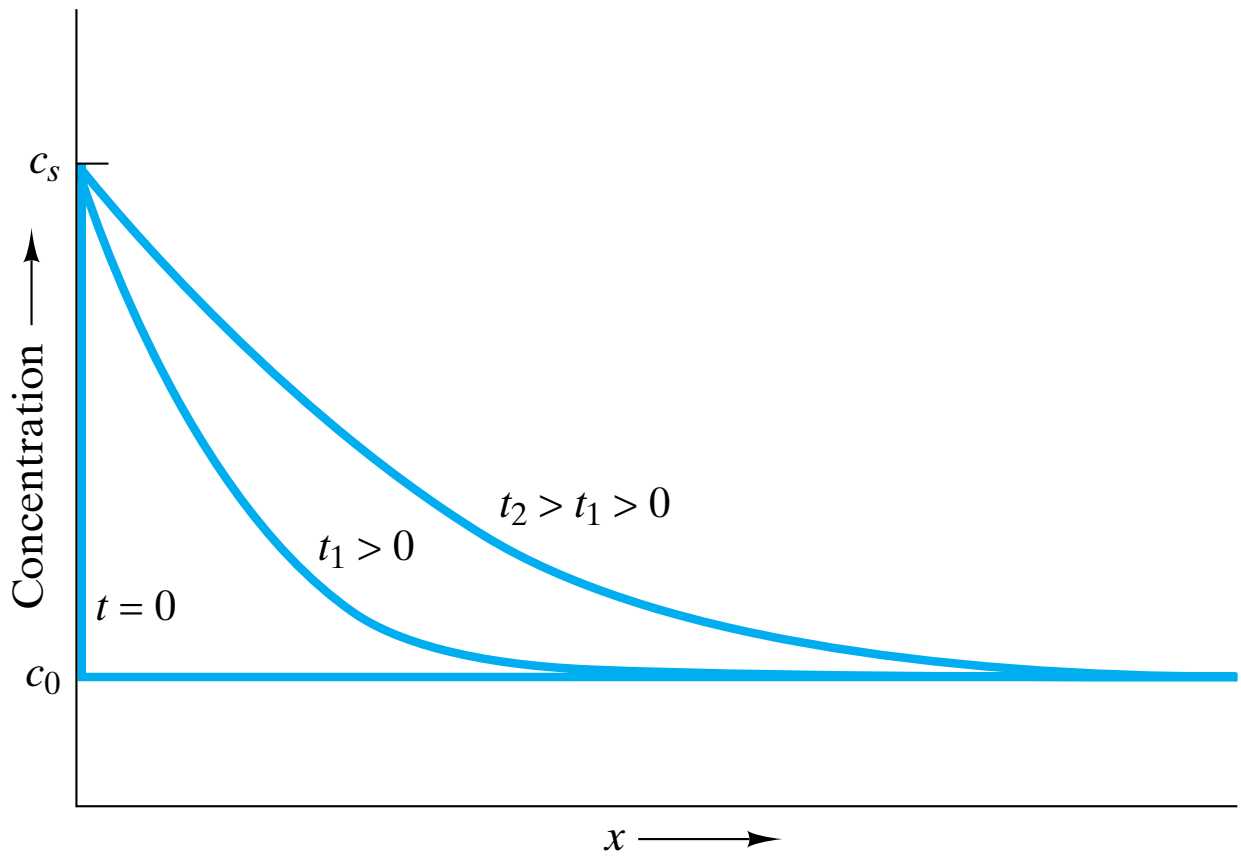


**Figure 5-10** Solution to Fick's second law (Equation 5.10) for the case of a semi-infinite solid, constant surface concentration of the diffusing species  $c_s$ , initial bulk concentration  $c_0$ , and a constant diffusion coefficient  $D$ .

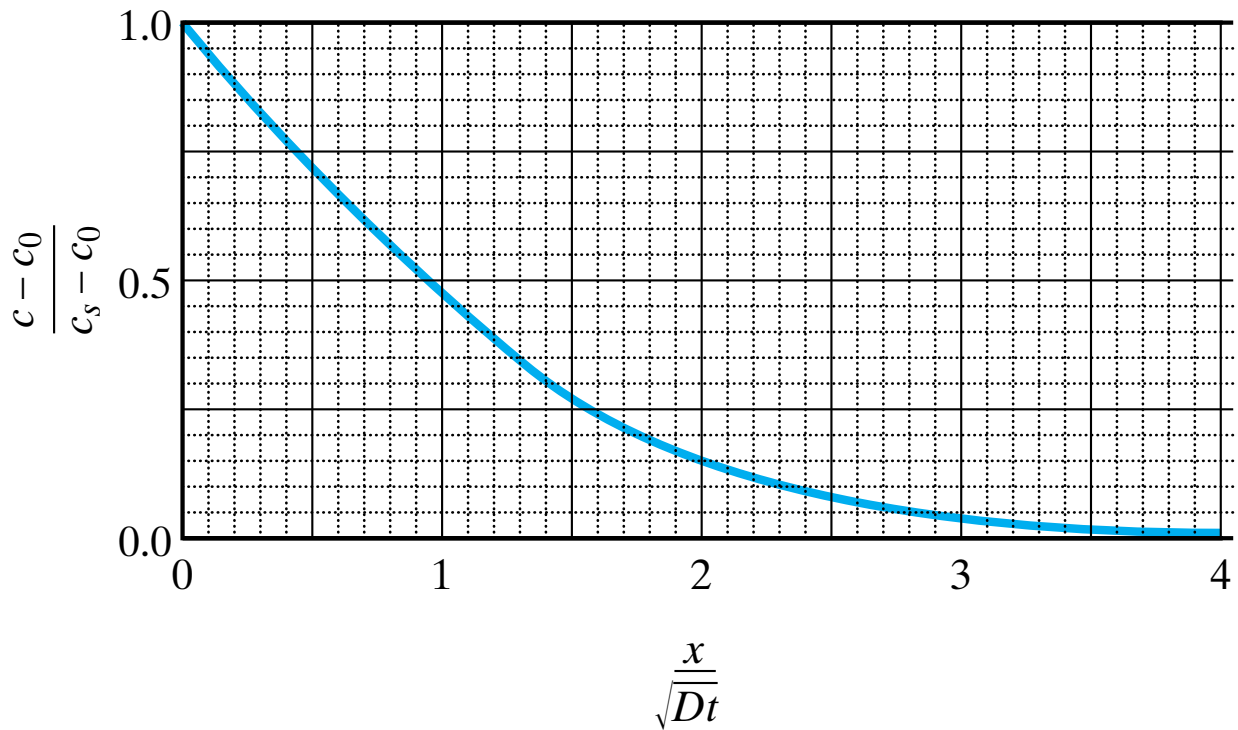


**Figure 5-11** Master plot summarizing all of the diffusion results of Figure 5-10 on a single curve.

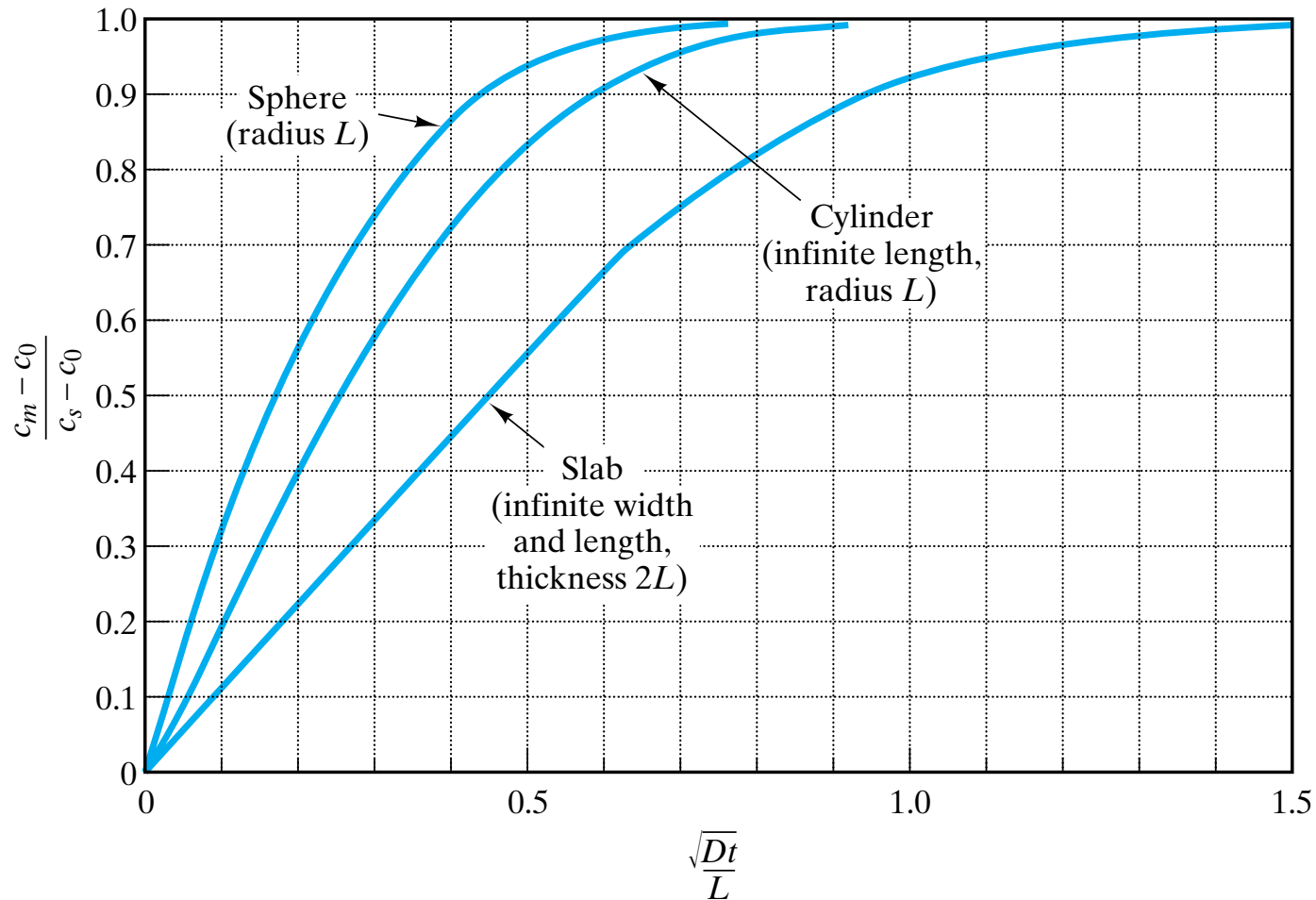


**Figure 5-12** Saturation curves similar to Figure 5-11 for various geometries. The parameter  $c_m$  is the average concentration of diffusing species within the sample. Again, the surface concentration  $c_s$  and diffusion coefficient  $D$  are assumed to be constant. (From W. D. Kingery, H. K. Bowen, and D. R. Uhlmann, *Introduction to Ceramics*, 2nd ed., John Wiley & Sons, Inc., New York, 1976.)

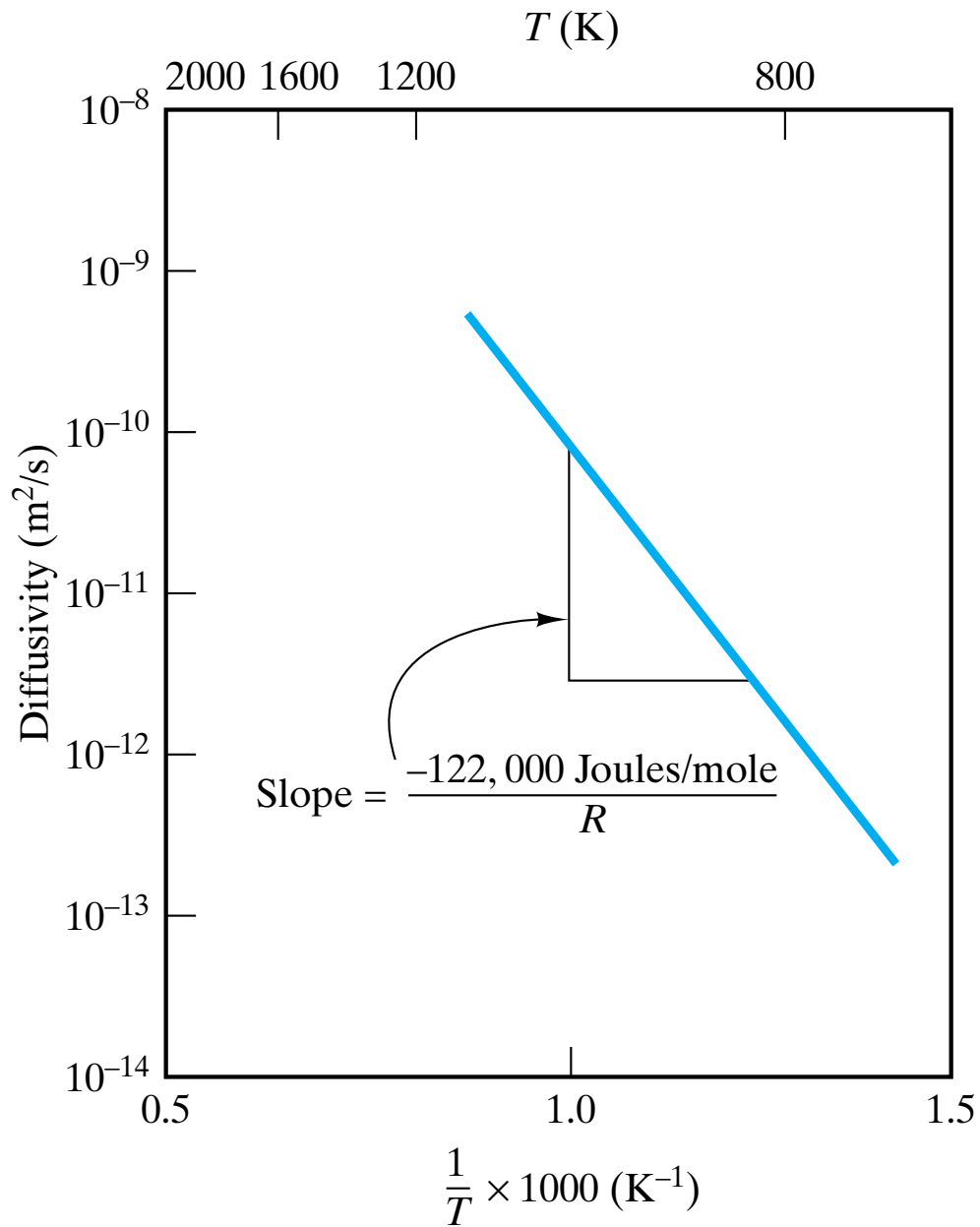


**Figure 5-13** Arrhenius plot of the diffusivity of carbon in  $\alpha$ -iron over a range of temperatures. Note also related Figures 4-4 and 5-6 and other metallic diffusion data in Figure 5-14.

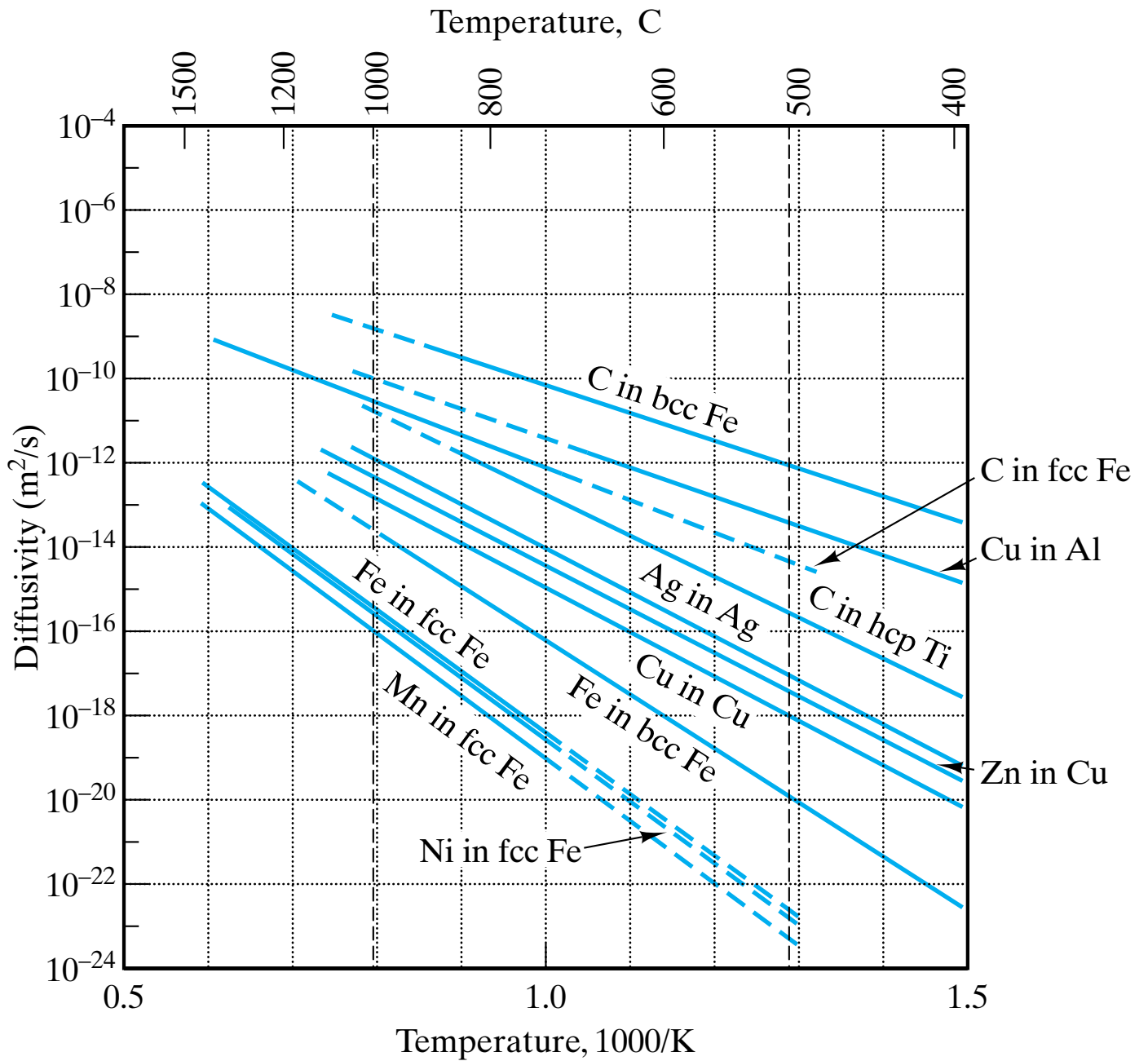


**Figure 5-14** Arrhenius plot of diffusivity data for a number of metallic systems. (From L. H. Van Vlack, *Elements of Materials Science and Engineering, 4th ed.*, Addison-Wesley Publishing Co., Inc., Reading, Mass., 1980.)

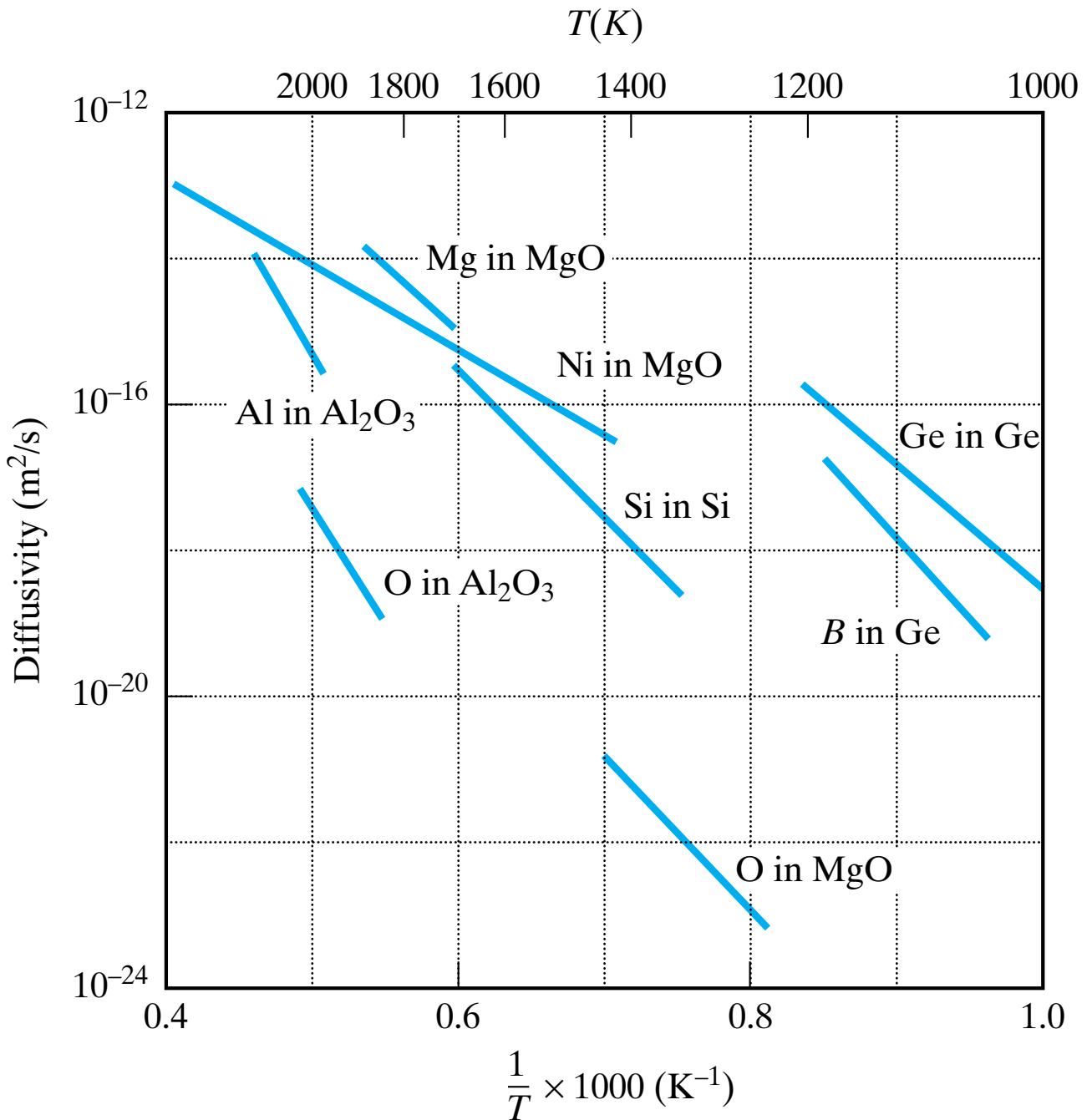


**Figure 5-15** Arrhenius plot of diffusivity data for a number of nonmetallic systems. (From P. Kofstad, *Nonstoichiometry, Diffusion, and Electrical Conductivity in Binary Metal Oxides*, John Wiley & Sons, Inc., New York, 1972; and S. M. Hu in *Atomic Diffusion in Semiconductors*, D. Shaw, ed., Plenum Press, New York, 1973.)

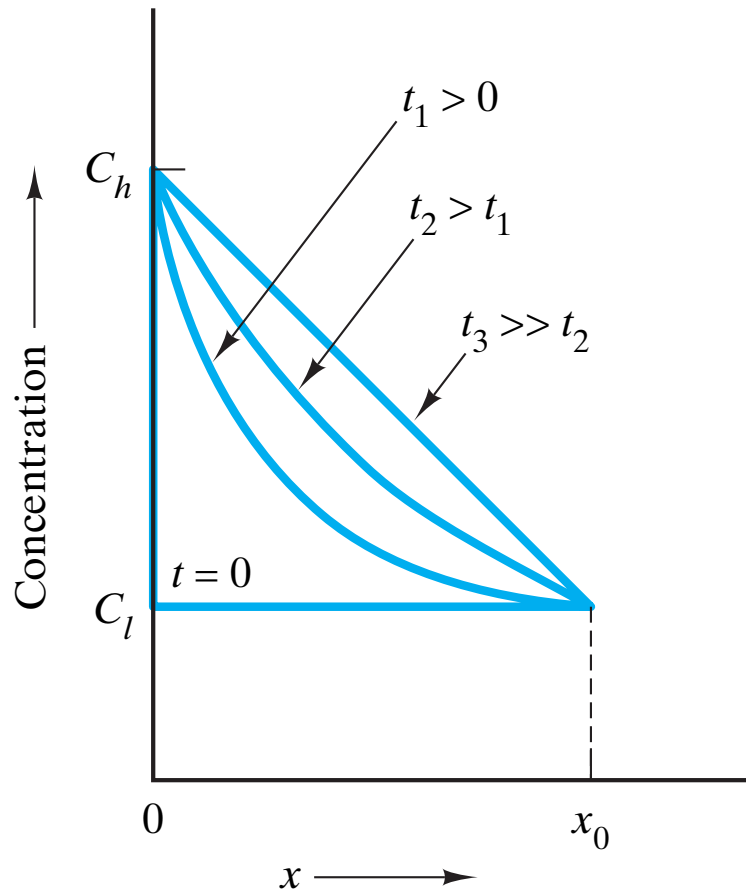
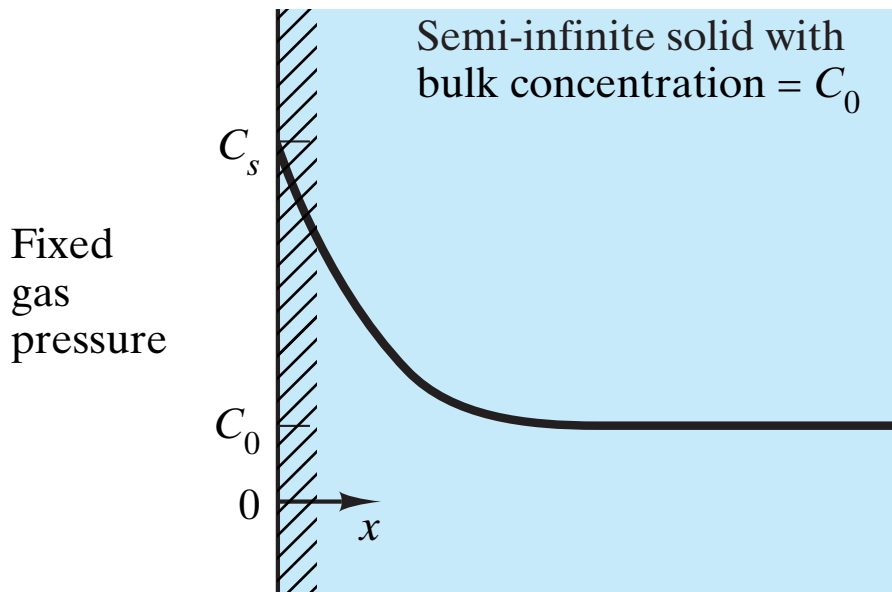
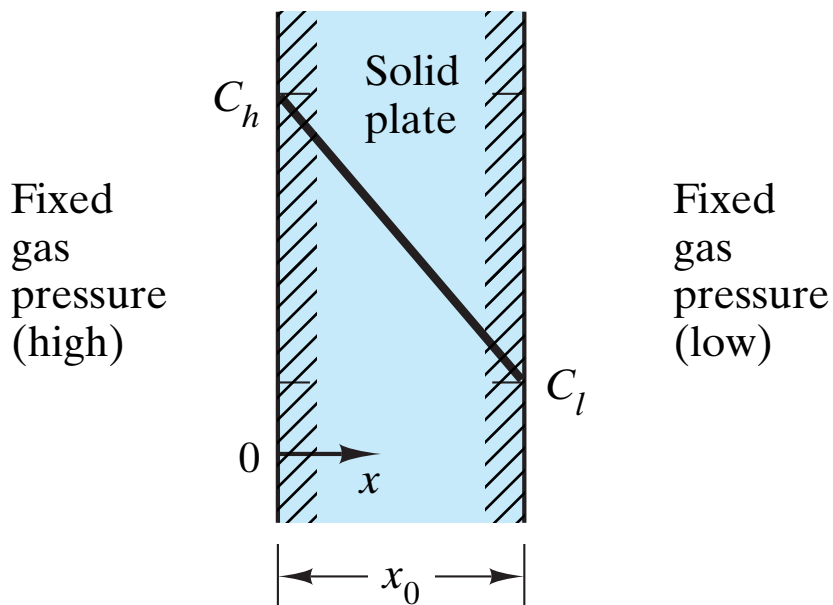


**Figure 5-16** Solution to Fick's second law (Equation 5.10) for the case of a solid of thickness  $x_0$ , constant surface concentrations of the diffusing species  $c_h$  and  $c_l$ , and a constant diffusion coefficient  $D$ . For long times, e.g.,  $t_3$ , the linear concentration profile is an example of steady-state diffusion.



(a)



(b)

**Figure 5-17** Schematic of sample configurations in gas environments that lead, after a long time, to the diffusion profiles representative of (a) non-steady state diffusion (Figure 5-10) and (b) steady-state diffusion (Figure 5-16).

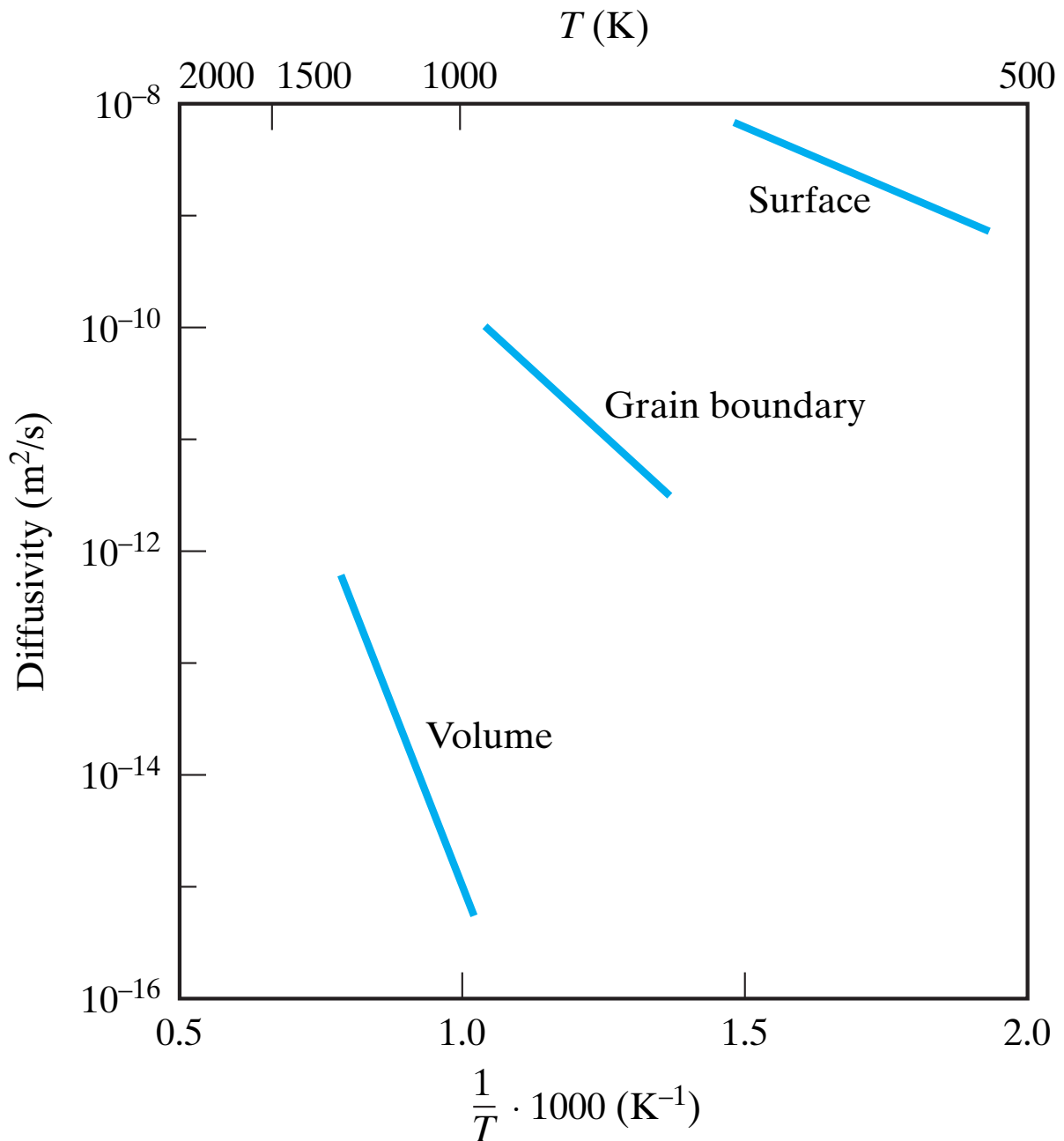


**Figure 5-18** Self-diffusion coefficients for silver depend on the diffusion path. In general, diffusivity is greater through less restrictive structural regions. (After J. H. Brophy, R. M. Rose, and J. Wulff, *The Structure and Properties of Materials, Vol. 2: Thermodynamics of Structure*, John Wiley & Sons, Inc., New York, 1964.)

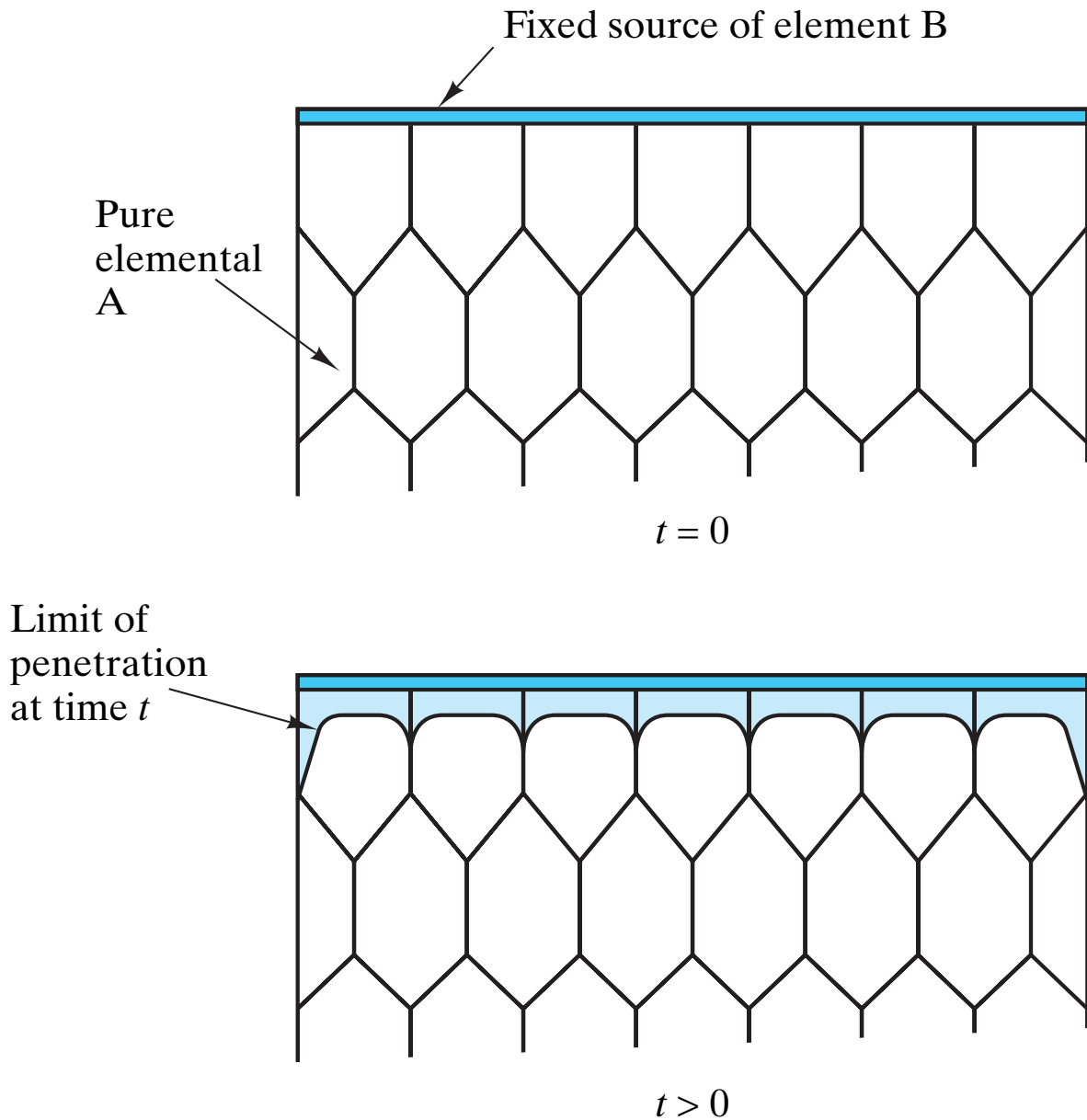


**Figure 5-19** Schematic illustration of how a coating of impurity *B* can penetrate more deeply into grain boundaries and even further along a free surface of polycrystalline *A*, consistent with the relative values of diffusion coefficients ( $D_{\text{volume}} < D_{\text{grain boundary}} < D_{\text{surface}}$ ).